Inhibition of Amyloid Fibril Formation and Cytotoxicity by Hydroxyindole Derivatives†

Tomer Cohen, Anat Frydman-Marom, Meirav Rechter, and Ehud Gazit*

Department of Molecular Microbiology and Biotechnology, George S. Wise Faculty of Life Sciences, Tel Aviv University, Tel Aviv 69978, Israel

Received August 1, 2005; Revised Manuscript Received February 28, 2006

ABSTRACT: Gaining insight into the mechanism of amyloid fibril formation, the hallmark of multiple degenerative syndromes of unrelated origin, and exploring novel directions of inhibition are crucial for preventing disease development. Specific interactions between aromatic moieties were suggested to have a key role in the recognition and self-assembly processes leading to the formation of amyloid fibrils by several amyloidogenic polypeptides, including the β-amyloid polypeptide associated with Alzheimer's disease. Our finding of the high-affinity molecular recognition and intense amyloidogenic potential of tryptophan-containing peptide fragments led to the hypothesis that screening for indole derivatives might lead to the identification of potential inhibitors of amyloid formation. Such inhibitors could mediate specific recognition processes without allowing further growth of the well-ordered amyloid chain. Using fluorescence spectroscopy, atomic force microscopy, and electron microscopy to screen 29 indole derivatives, we identified three potent inhibitors: indole-3-carbinol (I3C), 3-hydroxyindole (3HI), and 4-hydroxyindole (4HI). The latter, a simple low-molecular weight aromatic compound, was the most effective, completely abrogating not only the formation of aggregated structures by Aβ but also the cytotoxic activity of aggregated Aβ toward cultured cells. The results of this study provide further experimental support for the paradigm of amyloid inhibition by heteroaromatic interaction and point to indole derivatives as a simple molecular platform for the development of novel fibrillization inhibitors.

Alzheimer's disease (AD),[1] the most common cause of age-related dementia affecting ~20 million persons worldwide (*1*), is characterized by an extracellular accumulation of β-amyloid peptide (Aβ) in plaques composed mainly of the 42-amino acid polypeptide form and an intracellular appearance of neurofibrillary tangles (*1*−*3*). Although several biochemical and genetic studies have previously suggested that the formation of amyloid fibrils by Aβ protein has a central role in the pathogenesis of AD, the mechanism by which amyloid fibrils cause neuronal damage in vivo is not yet fully clear (*4*). In recent years, findings that early intermediates leading to the formation of amyloid fibrils are the most toxic assemblies are increasingly appreciated. Although early studies assumed that the insoluble large fibrillar aggregates of amyloid polypeptides are the cytotoxic agents (*5*−*7*), the results of more recent studies suggest that the most cytotoxic forms of amyloid proteins are the soluble oligomeric forms (*8*−*19*). The notion that the early, soluble intermediates are the key agents in the cytotoxic effect causing neuronal death and consequent dementia suggests that a major effort should be directed toward inhibiting amyloid formation at very early stages. Therefore, agents that target the basic molecular recognition process preceding the formation of early intermediates would be the most valuable.

Peptide array analysis revealed that a peptide fragment of Aβ as short as a pentapeptide, KLVFF, specifically binds to the full-length Aβ polypeptide (*20*). The formation of well-ordered amyloid fibrils from a seven-amino acid fragment of Aβ, KLVFFAE, has also been demonstrated (*21*). Other studies have shown that QKLVFF (*15*), LVFFA (*22*), LPFFD (*23*), and FFVLK (*24*) peptides are potent inhibitors of Aβ-fibril formation. Taken together, these findings suggest that the pair of the aromatic phenylalanine residues probably mediate the binding of the short peptide to the full-length Aβ polypeptide.

Several other studies have also suggested that aromatic interactions may have a role in the very early stages of amyloid formation, for example, by providing stability as well as order and directionality in the formation of amyloid fibrils (*25*), presumably facilitated by the restricted geometry of interaction between planar aromatic systems. Such ordered interactions between aromatic moieties are central in the self-assembly of complex biological and chemical supramolecular structures (*26*−*29*). In amyloidogenic peptide fragments, a high frequency of aromatic residues was observed. In addition, when aromatic moieties were replaced with other

† We acknowledge the financial support of the TAU-TECH technology partnership.

* To whom correspondence should be addressed: Department of Molecular Microbiology and Biotechnology, Tel Aviv University, Tel Aviv 69978, Israel. E-mail: ehudg@post.tau.ac.il. Telephone: +972-3-640-9030. Fax: +972-3-640-5448.

[1] Abbreviations: Aβ, amyloid-β polypeptide; AD, Alzheimer's disease; AFM, atomic force microscope or microscopy; DMSO, dimethyl sulfoxide; DMEM, Dulbecco's modified Eagle's medium; 3HI, 3-hydroxyindole; 4HI, 4-hydroxyindole; I3C, indole-3-carbinol; NMR, nuclear magnetic resonance; PBS, phosphate-buffered saline; TEM, transmission electron microscopy.

10.1021/bi051525c CCC: $33.50
Published on Web 03/25/2006

hydrophobic amino acids, a decrease in the amyloidogenic propensity was observed. These studies suggest a key role for aromatic moieties in many cases of amyloid formation (*21*, *25*, *30*−*35*). Recent studies using solid-state NMR (*36*) and X-ray and electron diffraction (*37*) provided high-resolution structural information about the role of aromatic interactions. The latter study is especially intriguing from this point of view as it provided information about the organization of aromatic moieties at the fibrillar form in atomic resolution. Additionally, theoretical studies, including a free-model analysis of a large set of amyloidogenic peptides, as well as molecular dynamic simulation, provide clear evidence for the importance of aromatic interactions in many cases of amyloid fibrillization (*38*−*43*). Another recent study scored the amyloidogenic propensity of phenylalanine and tryptophan to be 3 times higher than that of isoleucine and 6 times higher than that of valine (*44*). Very intriguingly, the aliphatic alanine and leucine were found to have negative propensity for amyloid formation.

In earlier studies, we demonstrated that modulating the aromatic nature of the islet amyloid polypeptide (IAPP) recognition motif significantly affects its amyloidogenic potential (*45*, *46*). The substitution of the central phenylalanine with tyrosine completely inhibited its amyloid formation (*45*). On the other hand, the modification of phenylalanine to tryptophan resulted in a fast and efficient self-association process of assemblies that differed from that of typical amyloid fibrils in their morphology (*45*). This result is in contrast to hydrophobic analogues that show very little if any aggregative behavior (*46*). A molecular recognition assay using peptide array analysis provided further insight into the system, suggesting that molecular recognition between hIAPP and its core amyloidogenic module is mediated by aromatic rather than by hydrophobic interactions (*46*). Although no recognition occurred between the full-length IAPP polypeptide and any phenylalanine to hydrophobic analogues, binding did occur with all three peptides containing natural aromatic analogues (the wild-type phenylalanine, tyrosine, or tryptophan). Binding to the tryptophan analogue was by far stronger than binding to the phenylalanine and tyrosine peptides (*46*). Moreover, it was recently reported that two indole derivatives, melatonin and indole-3-propionic acid (IPA), inhibit the formation of amyloid fibrils by Aβ. These compounds also have an antioxidant activity that may protect neurons from Aβ damage (*47*, *48*). The mechanism by which those three indole derivatives inhibit Aβ fibril formation is still unknown, and we cannot exclude the possibility of antioxidant activity. These observations together with our concept of heteroaromatic interactions as a direction for the inhibition of amyloid formation led us to examine tryptophan and indole analogues. We envisioned that indole derivatives could provide a novel direction toward identifying potential inhibitors that would not only allow high-affinity interaction at the very early stage of amyloid formation but also inhibit the further growth of typical amyloid fibrils.

In this work, we screened 29 indole derivatives for their ability to prevent the Aβ polypeptide from forming amyloid fibrils. Comparing such a diverse group of indole derivatives provided novel insight into the structural rules that direct the inhibition process.

EXPERIMENTAL PROCEDURES

Aβ and Indole Derivative Solutions. Synthetic lyophilized Aβ1−40 or Aβ1−42 (Bachem, Bubendorf, Switzerland) was dissolved in dimethyl sulfoxide (DMSO) to a concentration of 100 μM and sonicated for 1 min to prevent preaggregation. Aβ solutions were prepared by immediate dilution with 10 mM phosphate-buffered saline [100 mM NaCl and 0.5 mM EDTA (pH 7.4)] to a final concentration of 10 μM [containing 10% (v/v) DMSO].

The following indole derivatives were supplied by Sigma-Aldrich Inc.: indole-3-carbynol, tryptamine, 5-nitroindole, 7-methylindole, 5-methylindole, 3-methylindole, indolebutyric acid, indole-3-acetic acid, indole-6-carboxylic acid, indole-5-carboxylic acid, indole-3-carboxylic acid, indole-2-carboxylic acid, 2-indolinone, 3-hydroxyindole, 4-hydroxyindole, 5-hydroxyindole, Fmoc-D-Trp, Boc-L-Trp-OH, CBZ-D-tryptophanamide, CBZ-L-tryptophanamide, L-5-hydroxytryptophan, D-tryptophan, L-Tryptophan, indole-3-propionic acid, indole-3-ethanol, indole, Nα-Boc-D-Trp, Nα-Boc-L-Trp, and Fmoc-Trp-OH. The indole derivatives were dissolved in DMSO to a concentration of 20 mM and then diluted with 10 mM PBS buffer [100 mM NaCl and 0.5 mM EDTA (pH 7.4)] to a final concentration of 100 μM [containing 0.5% (v/v) DMSO].

ThT Binding Fluorescence. A 10 μM Aβ solution (either Aβ1−40 or Aβ1−42) was immediately mixed with the indole derivative stock solutions (100 μM) to a final Aβ concentration of 5 μM and various indole derivative concentrations. The samples were incubated at 37 °C, and the fibrillogenesis rate was monitored using ThT fluorescence analysis. The respective excitation and emission wavelengths were 450 nm (2.5 nm slit) and 480 nm (5 nm slit). A 10-fold diluted sample was taken and mixed with 900 μL of 0.4 μM ThT. The fluorescence of ThT was measured using a Jobin Yvon Horiba Fluoromax 3 fluorimeter. Each experiment was repeated in quadruplicate.

Fluorescence Polarization. 4HI was dissolved in dimethyl sulfoxide (DMSO) to a concentration of 50 nM and sonicated for 5 min. The solution was immediately mixed with increasingly larger aliquots of an Aβ1−42 stock solution (20 μM) to varying final polypeptide concentrations. 4HI polarization measurements were carried out using an ISS K2 fluorometer. The solutions were exited at 280 nm, and emission was monitored at 350 nm. For each single point, at least five measurements were collected and their average values were used for calculation. All experiments were performed in PBS (pH 7.4).

Transmission Electron Microscopy. A 10 μL sample from the Aβ1−40 ThT fluorescence assay was placed on a 400 mesh copper grid covered by carbon-stabilized Formvar film (SPI Supplies, West Chester, PA). After the mixture was allowed to stand for 1.5 min, excess fluid was removed and the grids were negatively stained for 2 min with 10 μL of a 2% uranyl acetate solution. Excess fluid was removed, and the samples were viewed using a JEOL 1200EX electron microscope operating at 80 kV.

Atomic Force Microscopy. A 60 μL sample from the Aβ1−40 ThT fluorescence assay was taken for AFM measurement at three different time points correlating to the amyloidogenic kinetic curve. The sample was centrifuged for 1.5 min at 13 000 rpm, and 40 μL of the supernatant

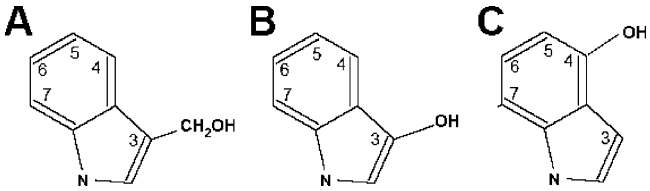

FIGURE 1: Structures of the most effective inhibitors identified in our screen: (A) indole-3-carbinol (I3C), (B) 3-hydroxyindole (3HI), and (C) 4-hydroxyindole (4HI).

was removed. The remaining 20 μL droplet of the solution was resuspended and deposited onto freshly cleaved mica for 1.5 min. The substrate was washed with 160 μL of double-distilled H_2O to reduce background and to eliminate salts and buffer contaminants, and the mica samples were dried at room temperature. At least four regions of the mica surface were examined to ensure that similar structures existed throughout the sample. AFM images were obtained using a Veeco NanoScope IV MultiMode AFM (Digital Instruments, Santa Barbara, CA) in tapping mode. Measurements were performed at a resonance frequency of ~321.4 kHz.

Cell Culture. The PC12 pheochromocytoma cell line was routinely grown in Dulbecco's modified Eagle's medium (DMEM) supplemented with 8% (v/v) fetal calf serum, 8% (v/v) horse serum, 100 units/mL penicillin, 100 units/mL streptomycin, and 2 mM L-glutamine (Biological Industries). The cells were maintained at 37 °C in a humidified atmosphere containing 5% CO_2.

Cell Cytotoxicity Assay. PC-12 cells (3×10^5 cells/mL) were cultured in 96-well microplates (100 μL/well) and incubated overnight at 37 °C. The wells were washed once with serum-free DMEM to exclude the effect of the serum. To each well was added 100 μL of 5 μM Aβ1−40 (prepared from a 0.5 mM stock solution in 10 mM NaOH) with the inhibitors at various concentrations. Each determination was made in quadruplicate. Following incubation for 24 h at 37 °C, cell viability was evaluated using the MTT assay (*49*). Twenty-five microliters of 5 mg/mL MTT dissolved in PBS was added to each well. After incubation for 4 h at 37 °C, 100 μL of extraction buffer [20% SDS dissolved in 50% dimethylformamide and a 50% DDW solution (pH 4.7)] was added to each well, and the plates were incubated again overnight at 37 °C. Finally, color intensity was measured using an ELISA reader at 570 nm.

RESULTS

Compounds Inhibiting Amyloid Aggregation. The inhibition potential of 29 different analogues was determined using the ThT fluorescence assay to measure the amount of amyloid fibrils after the addition of a fixed concentration of each compound. From the derivatives that were tested, the screen revealed three compounds that significantly inhibited the aggregation of Aβ1−42: indole-3-carbinol (I3C), 3-hydroxyindole (3HI), and 4-hydroxyindole (4HI) (Figure 1). Interestingly, the unmodified indole did not inhibit the aggregation of Aβ1−42. Other compounds, including 3-methylindole, indole-3-ethanol, indole-3-propionic acid, and 5-hydroxyindole, also showed no significant inhibition.

Concentration Dependence of Indole Inhibitors. To examine the inhibition efficiency of the three inhibitors, we studied the concentration dependence of inhibition of fibril formation (Figure 2). The fibrillization of Aβ1−42, with and without inhibitors, was assessed using the ThT fluorescence assay at a fixed incubation time of 24 h. The 3HI and 4HI compounds clearly showed a pattern of dose-dependent inhibition. I3C inhibited the fibrillization of Aβ1−42 only at high concentrations and showed no dose dependency. The IC_{50} of each inhibitor was calculated by the curve equation, and apparent IC_{50} values of ~85, ~100, and 200 μM were determined for 4HI, 3HI, and I3C, respectively.

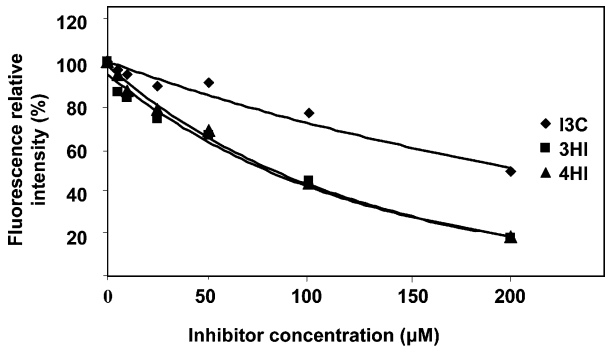

FIGURE 2: Concentration-dependent inhibition of Aβ1−42 fibrillogenesis. The inhibitors were added at different concentrations to a fixed amount of 5 μM Aβ1−42. After incubation for 24 h at 37 °C, ThT fluorescence was monitored at an emission wavelength of 480 nm (excitation at 450 nm). Samples contained different concentrations of I3C (◆), 3HI (■), and 4HI (▲).

We conducted a control experiment to rule out the possibility that the low values in the ThT fluorescence assay might result from a quenching effect by the inhibitor. Different concentrations of the three inhibitors were added to form Aβ1−42 fibrils, and fluorescence was immediately measured. No significant quenching effect was observed (data not shown).

Kinetics of Aβ1−40 Fibrillogenesis Inhibition. After examining the inhibitory effect of the three inhibitors on the Aβ1−42 fibrillogenesis at the end point, we studied their effect on the kinetics of fibrillogenesis. To obtain better temporal resolution, we used Aβ1−40 because it has a slower fibrillogenesis rate (*50*), assuming that a slower rate would allow more significant inhibition and a better understanding of the effect. The inhibitors were added at concentrations of 5, 25, and 50 μM to a solution containing 5 μM Aβ1−40, and the inhibition of the kinetics of Aβ1−40 fibrillogenesis was assessed (Figure 3).

The ThT fluorescence curve exhibited a characteristic sigmoid shape representing three phases: the nucleation phase (lag phase), the polymerization phase, and the equilibrium phase (stationary phase). The samples containing 25 and 50 μM 4HI showed a significantly longer nucleation phase, which persisted for the duration of the measurements (Figure 3). In the sample containing 5 μM 4HI, the effect on the nucleation phase was less significant. The samples containing 3HI and I3C had no effect on the nucleation phase when compared with the control (Figure 3).

All three compounds were inhibitory in the polymerization phase, and all changed the slope of the curve, but with different magnitudes. I3C had an effect on the slope of the growth curve only at 50 μM and had no effect at lower concentrations. 3HI exhibited a dose-dependent effect, in which the slope of the growth curve changed in parallel with increasing concentrations of 3HI. The slope of the samples

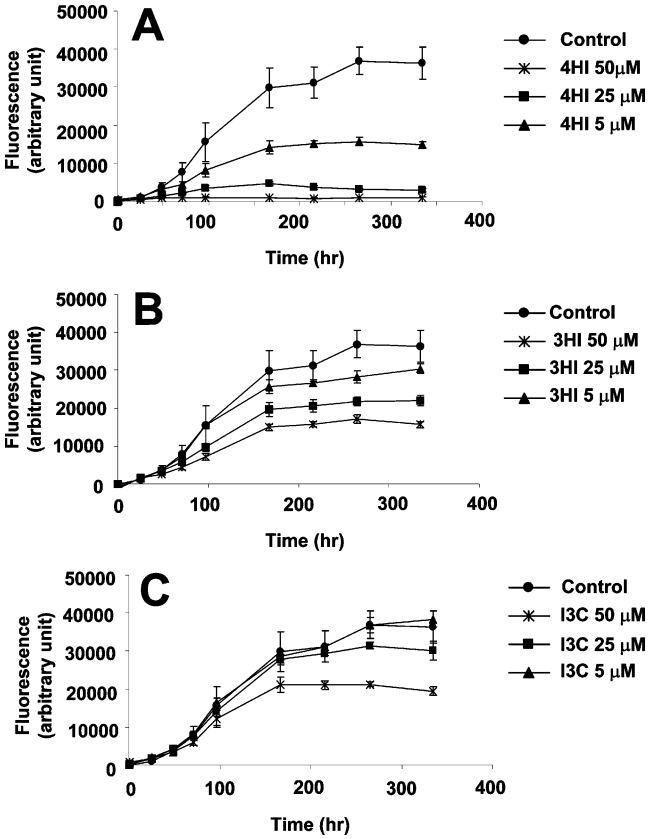

FIGURE 3: Kinetics of Aβ1−40 fibrillogenesis. Inhibitors were added to a fixed concentration of 5 μM Aβ1−40. Three concentrations of inhibitors were used: 5 (▲), 25 (■), and 50 μM (s★). The kinetics of fibril aggregation were measured for 14 days using the ThT fluorescence assay on incubated samples containing 4HI (A), 3HI (B), and I3C (C). The wild-type sample (∗) served as a control to which no inhibitor was added.

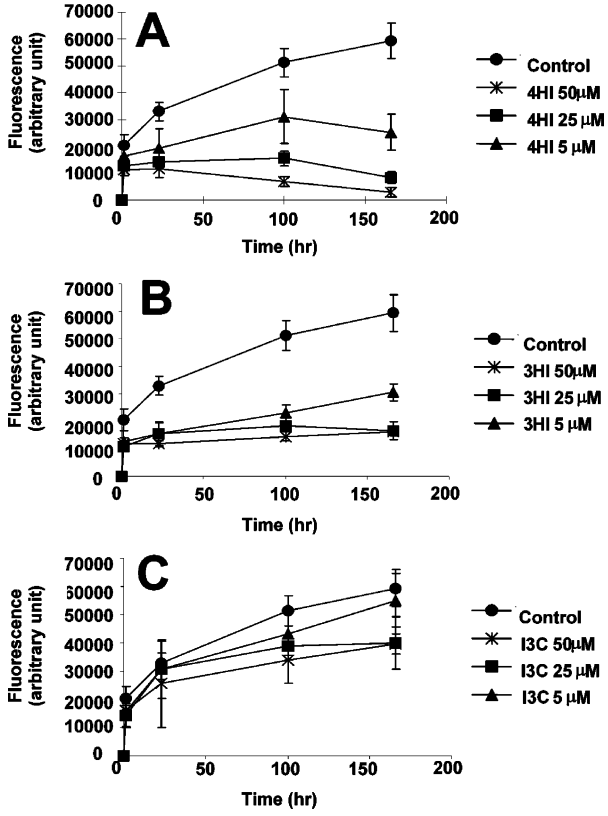

FIGURE 4: Kinetics of Aβ1−40 fibrillogenesis. Inhibitors were added to a fixed concentration of 5 μM Aβ1−40 when the fibrillogeneses had already started. Three concentrations of inhibitors were used: 5 (▲), 25 (■), and 50 μM (∗). The kinetics of fibril aggregation were measured for 14 days using the ThT fluorescence assay on incubated samples containing 4HI (A), 3HI (B), and I3C (C). In the control sample (●), no inhibitor was added.

containing 5 μM 4HI was sharper than that of the control or of other inhibitors.

Differences in the level of ThT fluorescence at equilibrium are influenced by the ability of the inhibitor to redirect the Aβ away from the polymerization pathway. At the final equilibrium phase at the end point of the experiments, 4HI was the most effective inhibitor at all three concentrations. The inhibition level at 5 μM was close to 60% and was almost complete at 25 and 50 μM. The addition of 25 μM 3HI led to an inhibition of ∼40%, which rose to ∼60% at 50 μM. Finally, the addition of 50 μM I3C resulted in a decrease of almost 50%.

To gain further insights with regard to the fibrillogenesis phase in which the inhibitors are effective, we performed another kinetic assay. In this assay, the different concentrations of the three indole derivatives were added to Aβ_{1-40} samples after the nucleation phase reached completion and the fibrillogenesis had already started.

All three compounds inhibited the polymerization phase, and all changed the slope of the curve, but with different magnitudes. I3C had an effect on the slope of the growth curve only at 50 μM and had no effect at lower concentrations. The samples containing 25 and 50 μM 3HI exhibited a complete block of the polymerization phase. The samples containing 4HI exhibited not only a slower polymerization rate but also a decrease in the ThT measurement at equilibrium (Figure 4). At the final equilibrium phase at the

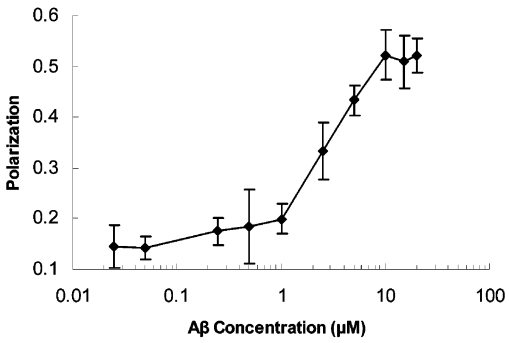

FIGURE 5: Fluorescence polarization analysis of the 4HI−Aβ interaction. Complex formation was monitored via the fluorescence polarization of 4-hydroxyindole upon titration with an Aβ solution. The concentration of the 4HI was 50 nM. The excitation wavelength was 280 nm, and polarization was monitored at 350 nm.

end point of the experiments, 4HI was the most effective inhibitor at all three concentrations. The inhibition level at 5 μM was close to 60% and was almost complete at 25 and 50 μM. The addition of 5 μM 3HI led to an inhibition of ∼50%, which rose to ∼70% at 25 or 50 μM. Finally, the addition of 25 or 50 μM I3C resulted in a decrease of almost 30%.

Binding Affinity. To determine the affinity of the interaction between 4HI and Aβ1−42, we monitored changes in the fluorescence polarization values of the indole fluorophore at different 4HI:Aβ molar ratios (Figure 5). Half-maximal binding occurred at an Aβ concentration of ∼3 μM (Figure

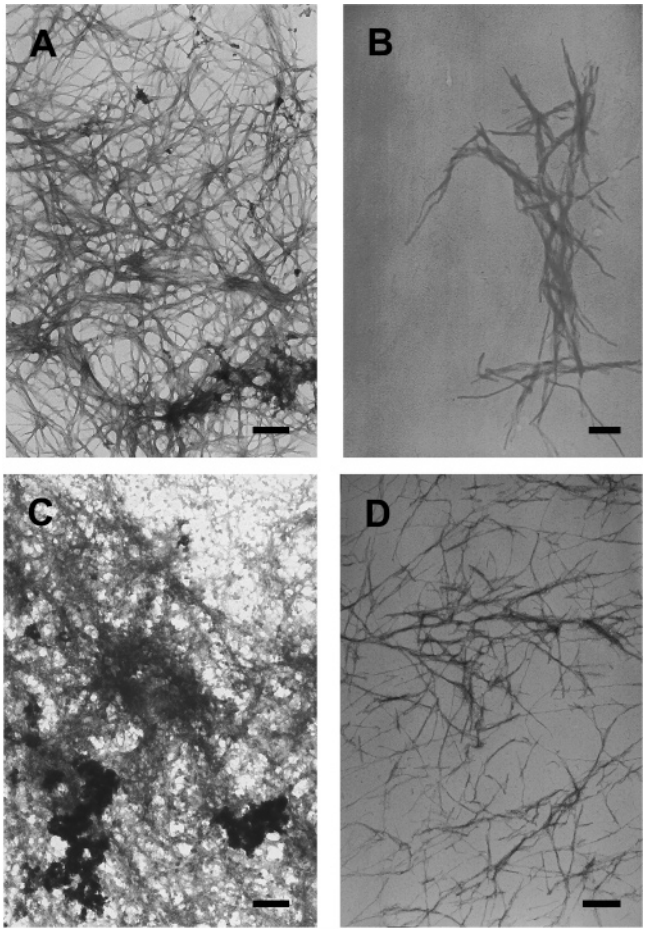

FIGURE 6: TEM micrographs of aggregated samples after incubation for 7 days. The samples were negatively stained using 2% uranyl acetate. (A) Control sample containing Aβ1−40 in PBS. (B−D) Samples containing Aβ1−40 in the presence of 25 μM 4HI (B), 50 μM 3HI (C), or 50 μM I3C (D). The scale bar represents 200 nm.

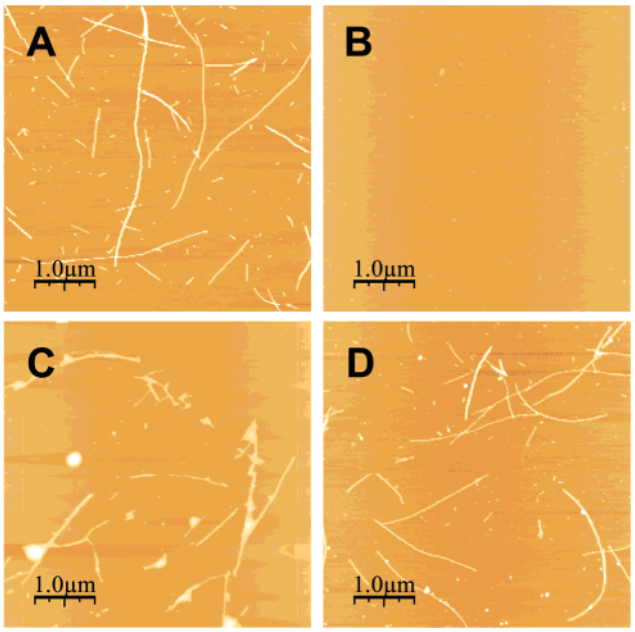

FIGURE 7: AFM height images (5 μm × 5 μm) of Aβ1−40 aggregates deposited on mica following inhibition by different indole derivatives. AFM samples were taken when ThT fluorescence indicated that control samples containing Aβ1−40 alone in PBS had reached the polymerization phase. (A) Control sample. (B−D) Samples containing Aβ1−40 in the presence of 50 μM 4HI (B), 50 μM 3HI (C), or 50 μM I3C (D). When the ThT assay indicated that the control samples had reached the equilibrium phase, other AFM samples were deposited and imaged.

5). Since the concentration of 4HI (50 nM) was significantly lower than that of Aβ, at the concentrations at which a large degree of binding occurred, we can assume that the concentration of free Aβ did not differ much from that of the total Aβ. Therefore, under these assumptions, we can assume a K_d of ~3 μM to monomeric Aβ. This K_d represents an upper limit for the affinity, due to the fact that if the basic binding unit is not a monomer but rather a small oligomer, the apparent K_d will have a sub-micromolar value.

Ultrastructural Analysis of Aggregation. To determine the effect of the inhibitory compounds on the ultrastructural properties of the assembled Aβ, we first performed TEM analysis on samples of Aβ1−40 from the kinetic assay after incubation for 14 days and on samples of Aβ1−42 from the dose-dependent assay after 24 h. The control samples of Aβ1−40 contained abundant amyloid fibrils aggregated in PBS (Figure 6A), whereas samples containing Aβ1−40 and 25 μM 4HI were devoid of fibrils and contained only a very small amount of small fibrils (Figure 6B). In the samples containing Aβ1−40 and 50 μM 4HI, almost no fibrils were observed on the EM grid. The EM grids with 50 μM 3HI had a significant number of amorphous aggregates showing a congested form that might affect ThT measurements because of binding (Figure 6C). The I3C sample contained Aβ1−40 aggregates in the same form that was observed in the control sample but in smaller amounts (Figure 6D). When TEM analysis was preformed with the Aβ1−42 samples, aggregates of amyloid fibrils were observed in all EM grids.

AFM analysis of Aβ1−40 samples taken from the kinetic experiment after the control samples reached the different fibrillogenesis phase revealed that no sample analyzed immediately exhibited amyloid fibrils (data not shown). Examination of the samples after the control samples reached the polymerization phase showed different levels of amyloid fibril formation. Small amounts of amyloid fibrils in the form of long wires were seen in the control and I3C samples (Figure 7A,D), whereas samples containing Aβ1−40 and 4HI showed no fibrils (Figure 7B). 3HI exhibited different fibril morphology and created small aggregates that interacted with the amyloid fibrils (Figure 7C).

Inhibition of the Cytotoxic Effect of Amyloid-β Peptide in PC12 Cells. We studied the effect of the inhibitors on the formation of cytotoxic amyloid assemblies by measuring the toxicity of Aβ on pheochromocytoma cell line cultures (PC12) in the presence and absence of the three inhibitors. The inhibitors were mixed with 5 μM Aβ1−40 at different concentrations and the solutions added to the cells at two time points: immediately ($T = 0$) or after incubation for 7 days. Cell viability was determined after 24 h using the MTT assay. The $T = 0$ results represent the cytotoxic effect during the first 24 h of Aβ fibrillogenesis. The control treatment (cells incubated with only 5 μM Aβ1−40) survival rate was ~56% (Figure 8A). The $T = 7$ results represent the cytotoxic effect at the end point phase, when large and congested amyloid fibrils were already formed. The control treatment (cells incubated with only 5 μM Aβ1−40) survival rate in this assay (~74%) was higher than that at time zero (Figure

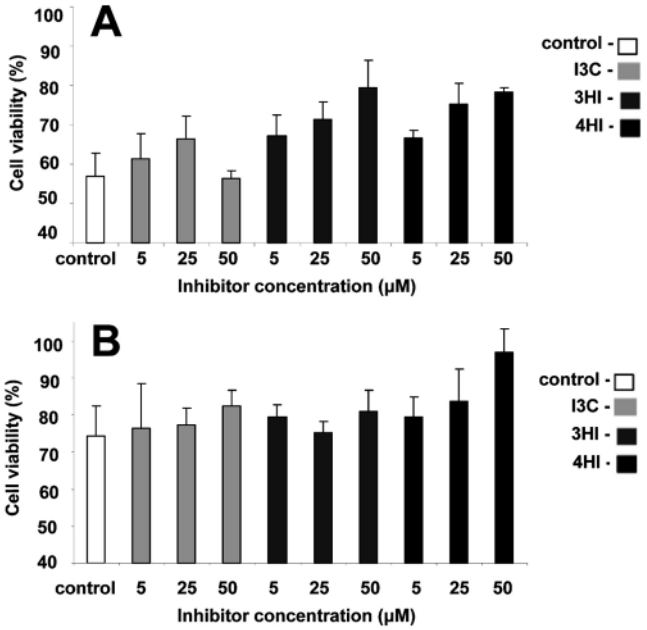

FIGURE 8: Cell culture assay. The three inhibitors (4HI, 3HI, and I3C) were preincubated at different concentrations with 5 μM Aβ1−40 forming a mixture of Aβ and inhibitor. PC12 cells were maintained in the absence or presence of the sample mixtures. Cell viability was determined using the MTT viability assay after 24 h. The sample mixtures were added at two time points: (A) immediately after the sample mixtures was made and (B) after incubation of the sample mixtures for 7 days.

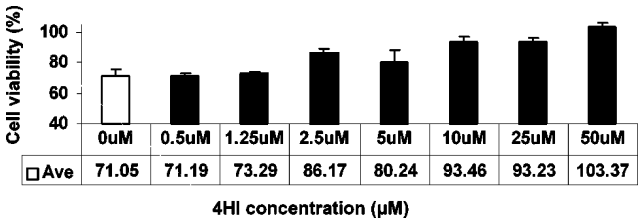

FIGURE 9: 4HI concentration-dependent cell culture assay. The 4HI inhibitor was added at different concentrations to a fixed amount of 5 μM Aβ1−40 and incubated for 7 days at 37 °C. PC12 cells were maintained in the absence or presence of this mixture. Cell viability was determined using the MTT viability assay after 24 h.

8B). Although all three compounds inhibited the fibril aggregation rate in the ThT assay, 4HI had the most significant inhibitory effect on Aβ1−40 cytotoxicity in both cell culture assays. When 25 or 50 μM 4HI was added to a solution containing Aβ1−40, the viability rate of PC12 cells was elevated by ∼25% when compared with that under control conditions (Figure 8A,B). In the presence of 3HI, the PC12 survival rate was improved by ∼25% only in the first assay (Figure 8A). I3C showed no significant inhibition of cytotoxicity in either assay. The inhibitors alone had no effect on the survival of PC12 cells in culture (data not shown). The protective effect of 4HI was further examined by adding different concentrations of 4HI to 5 μM Aβ1−40 and PC-12 cells. The cell viability assay was assayed after incubation for 7 days (Figure 9). The protective effect of 4HI exhibited dose−response behavior. The minimum concentration of 4HI required for significant inhibition was 2.5 μM, whereas the toxic effect of Aβ1−40 was completely blocked at 50 μM 4HI (Figure 9). A complete toxicity block was also shown when the cell culture assay was preformed with the Aβ1−42 peptide and 50 μM 4HI (data not shown).

DISCUSSION

Alzheimer's disease, like other neurodegenerative diseases, is associated with the formation of amyloid fibrils. Because the mechanism leading to the formation of well-ordered fibrils is not fully understood, the rational design of inhibitors is a complex task. Despite this information gap, by systematically screening 29 indole derivatives, we identified three small anti-amyloidogenic molecules that were highly effective in inhibiting amyloid fibril formation and cytotoxicity for cultured pheochromocytoma cells, a benign tumor of the sympathetic nervous system. The relatively high success rate reflects the results of prior experimental and theoretical studies revealing the apparent role of aromatic residues in the molecular recognition and self-assembly processes that lead to the formation of amyloid fibrils (*25*−*46*).

The results of the study presented here indicate that hydroxyindole derivatives are the most potent inhibitors of amyloid fibril formation by Aβ and its consequent cytotoxic effect. Examining other indole derivatives exhibiting little or no inhibitory effect is also extremely important for understanding the mechanism of inhibition. Careful examination of the noninhibitory compounds revealed that indole alone does not inhibit the process and requires a hydroxyl group to inhibit the formation of amyloid assemblies. Only indole derivatives having a hydroxyl group positioned on C3 and C4 showed significant inhibitory properties.

The hydroxyl group is an electron donor, and its integration results in an altered electron density and a negative charge on the benzopyrrole ring. Additionally, the hydroxyl group has the ability to interact with various moieties by a means of hydrogen bonds. The position of the hydroxyl group is of key importance, which became clearer when we examined indole derivatives containing only a methyl group in different positions. Such derivatives showed either an insignificant inhibitory effect or no inhibition according to their position on the benzopyrrole ring. The methyl group alone had an inductive effect on the benzopyrrole electrons, but this effect is minor compared with the hydroxyl group effect. When we examined different derivatives such as methyl or ethyl, in which a hydroxyl group was part of a steric group, no inhibition occurred when the hydroxyl group was more than one carbon away from the benzopyrrole. For example, I3C inhibited the reaction to a lower extent than 3HI and the indole-3-ethanol and indole-3-propionic acid failed to inhibit the formation of amyloid fibrils at all. The inhibitory mechanism of the compounds studied here remains unclear, but we assume that the hydroxyl group interacts with the backbone of the peptides and that the different electron density and negative charge on the benzopyrrole ring prevents the ability of another Aβ peptide to create a π-stacking interaction, hence blocking the extension of the fibrillogenesis process.

The nitrogen atom of the indole can participate in a NH$\cdot\cdot\cdot\pi$ hydrogen bond with the ring of another aromatic residue. The energy of this bond is near −2.81 kcal/mol (*51*). Therefore, it is a more favorable interaction than typical nonbonding aromatic−aromatic interactions which are on the order of 1−2 kcal/mol (*52*). It is not unlikely to assume that over the surface of an oligomer, which is composed of several Aβ peptides, there will be several NH$\cdots\pi$ hydrogen

binding sites. Therefore, the avidity of such interaction will be significantly increased.

Recent evidence indicates that the toxicities of Aβ and other amyloidogenic proteins lie in the soluble oligomeric forms (*8*−*19*). This understanding is supported by many in vitro and in vivo studies, leading to the notion that potential anti-amyloid compounds (*53*−*57*) should block the very early stages of amyloid oligomerization, most likely the cytotoxic stage. The kinetic assay was a first step in determining the phases inhibited by each identified compounds. The characteristic sigmoidal curve obtained in the ThT fluorescence assay is consistent with the nucleation-dependent polymerization model (*58*, *59*). An inhibitor changes the shape of the fibrillogenesis curve in three ways: (1) interference with nucleation, increasing the lag time; (2) interference during the polymerization step, which should slow its rate significantly; and (3) inhibition in which Aβ is diverted from the polymerization pathway, reducing the end point equilibrium level. The results of this study show that I3C and 3HI interfere in the polymerization stage and divert the process away from that pathway. 4HI seemed to interfere in all three steps. In correlation with quantitative fluorescence assays, qualitative microscopy analysis revealed that even after careful examination, the only grids showing no amyloid fibrils in the TEM analysis were those containing samples of Aβ with 5 μM 4HI. Additional powerful qualitative support emerged from the AFM analysis in which samples were examined in the three fibrillogenesis curve phases. All AFM samples were clear of fibrils in the immediate lag phase, and only those containing 4HI remained clear of amyloid fibrils in the polymerization phase. The results of AFM support those of the kinetic assay in which the 4HI lag time was longer than in other samples, suggesting that 4HI blocks Aβ fibrillogenesis in the early stages of nucleation. We observed an apparent paradox in the 3HI results, in which a significant decrease occurred in the Aβ fibrillogenesis kinetic assay with no improvement in the survival of cultured PC12 cells. The variant morphology among the amorphous aggregates shown in the TEM micrograph (Figure 6C) likely caused such a discrepancy. The cytotoxicity of those amorphous aggregates is unknown, and it is not unlikely that the differences in the 3HI inhibitory effect on cytotoxicity between the 1 day incubation PC12 cell culture assay and the 7 day incubation assay are due to their cytotoxicity. Therefore, on one hand, the 3HI blocked the Aβ cytotoxicity effect, and on the other hand, it causes amorphous toxic aggregates.

The mechanism by which amyloid fibrils cause neuronal death in vivo remains unclear, and a definitive correlation between fibrillar plaque density and the severity of dementia in Alzheimer's diseased brains has not always been found (*3*, *60*). This observation is consistent with the results of our cell culture assay, in which control samples incubated until the amyloid fibrillogenesis curve reached the end point phase were less toxic than those added immediately (Figure 8).

The results of both quantitative fluorescence assays and qualitative microscopy analyses indicate that 4HI was the only compound to inhibit Aβ fibril formation during post-nucleation phase initialization in a dose-dependent manner. The results, along with those of other studies claiming that any potential anti-amyloid compound can block Aβ oligomerization, the neurotoxic form, can explain why 4HI completely inhibited the toxicity of Aβ1−40 in both cell culture assays (Figure 8), whereas all three inhibitors decreased the fibril aggregation rate in the ThT assay. The method used to dissolve lyophilized Aβ in cell culture experiments differs from that used in ThT assays because DMSO is toxic for cells. This different dissolving method accelerated Aβ fibrillogenesis kinetics, which might explain the lower inhibition percentages of all three inhibitors in general and of 4HI in particular in the cell culture assay.

A lower inhibition percentage was also observed when we compared the Aβ1−40 and Aβ1−42 inhibition results. This might be explained by the different fibrillogenesis rates of the two polypeptides (*50*). We assume that a slower fibril formation rate allows better interaction between the inhibitor and the Aβ recognition motif in its monomeric or low-oligomeric state. The ability of the inhibitor to target these monomers and early assemblies probably results in much more significant inhibition.

The issue of the generic nature of indole derivatives to inhibit other amyloidogenic proteins is another major aspect that is needed to be studied. So far, only few small molecules were described as inhibitors of more than one amyloidogenic protein (*61*, *62*). Another study by our group demonstrated that the three indole derivatives have an inhibiting effect on other amyloidogenic proteins, including human calcitonin and the human islet amyloid polypeptide (IAPP) (data not published).

In summary, these findings indicate that simple indole derivatives such as 4HI, 3HI, and I3C effectively inhibit Aβ peptide-induced amyloid fibril formation and prevent cell death induced by the peptide in culture. The anti-amyloidogenic compounds described here, especially 4HI, should be considered lead compounds for the development of drugs to inhibit oligomerization and prevent the neurotoxicity of Aβ in Alzheimer's disease. Therefore, we recommend further in vivo study in which blood−brain barrier (BBB) permeability will be examined. The small size of the indole derivatives (molecular mass of ~135 Da), their hydrophobicity, and excellent BBB permeability of indole derivatives such melatonin and 5-hydroxy-L-tryptophan hint that they might actually have a high permeability rate.

ACKNOWLEDGMENT

We thank Dr. Shahcar Richtet for his help with the AFM experiments and Oren Oster for help with the ThT experiments. We thank members of the Gazit laboratory for helpful discussions.

REFERENCES

1. Haass, C., and De Strooper, B. (1999) The presenilins in Alzheimer's disease proteolysis holds the key, *Science 286*, 916−919.
2. Selkoe, D. J. (2002) Alzheimer's disease is a synaptic failure, *Science 298*, 789−791.
3. Buee, L., Bussiere, T., Buee-Scherrer, V., Delacourte, A., and Hof, P. R. (2000) Tau protein isoforms, phosphorylation and role in neurodegenerative disorders, *Brain Res. Rev. 33*, 95−130.
4. Caughey, B., and Lansbury, P. T., Jr. (2003) Protofibrils, pores, fibrils, and neurodegeneration: Separating the responsible protein aggregates from the innocent bystanders, *Annu. Rev. Neurosci. 26*, 267−298.
5. Pike, C. J., Burdick, D., Walencewicz, A. J., Glabe, C. G., and Cotman, C. W. (1993) Neurodegeneration induced by β-amyloid

peptides *in vitro*: The role of peptide assembly state, *J. Neurosci. 13*, 1676−1687.
6. Lorenzo, A., and Yankner, B. A. (1994) β-Amyloid neurotoxicity requires fibril formation and is inhibited by Congo red, *Proc. Natl. Acad. Sci. U.S.A. 91*, 12243−12247.
7. Grace, E. A., Rabiner, C. A., and Busciglio, J. (2002) Characterization of neuronal dystrophy induced by fibrillar amyloid β: Implications for Alzheimer's disease, *Neuroscience 114*, 265−273.
8. Lambert, M. P., Barlow, A. K., Chromy, B. A., Edwards, C., Freed, R., Liosatos, M., Morgan, T. E., Rozovsky, I., Trommer, B., Viola, K. L., Wals, P., Zhang, C., Finch, C. E., Krafft, G. A., and Klein, W. L. (1998) Diffusible, nonfibrillar ligands derived from Aβ1−42 are potent central nervous system neurotoxins, *Proc. Natl. Acad. Sci. U.S.A. 95*, 6448−6453.
9. Wang, H. W., Pasternak, J. F., Kuo, H., Ristic, H., Lambert, M. P., Chromy, B., Viola, K. L., Klein, W. L., Stine, W. B., Krafft, G. A., and Trommer, B. L. (2002) Soluble oligomers of β amyloid (1−42) inhibit long-term potentiation but not long-term depression in rat dentate gyrus, *Brain Res. 924*, 133−140.
10. Walsh, D. M., Klyubin, I., Fadeeva, J. V., Rowan, M. J., and Selkoe, D. J. (2002) Amyloid-β oligomers: Their production, toxicity and therapeutic inhibition, *Biochem. Soc. Trans. 30*, 552−557.
11. Kim, H. J., Chae, S. C., Lee, D. K., Chromy, B., Lee, S. C., Park, Y. C., Klein, W. L., Krafft, G. A., and Hong, S. T. (2003) Selective neuronal degeneration induced by soluble oligomeric amyloid beta protein, *FASEB J. 17*, 118−120.
12. Kayed, R., Head, E., Thompson, J. L., McIntire, T. M., Milton, S. C., Cotman, C. W., and Glabe, C. G. (2003) Common structure of soluble amyloid oligomers implies common mechanism of pathogenesis, *Science 300*, 486−489.
13. Lashuel, H. A., Hartley, D., Petre, B. M., Walz, T., and Lansbury, P. T., Jr. (2002) Neurodegenerative disease: Amyloid pores from pathogenic mutations, *Nature 418*, 291.
14. Porat, Y., Kolusheva, S., Jelinek, R., and Gazit, E. (2003) The human islet amyloid polypeptide forms transient membrane-active protofilaments, *Biochemistry 42*, 10971−10977.
15. Cleary, J. P., Walsh, D. M., Hofmeister, J. J., Shankar, G. M., Kuskowski, M. A., Selkoe, D. J., and Ashe, K. H. (2004) Natural oligomers of the amyloid protein specifically disrupt cognitive function, *Nat. Neurosci. 8*, 79−84.
16. Bitan, G., Fradinger, E. A., Spring, S. M., and Teplow, D. B. (2005) Neurotoxic protein oligomers: What you see is not always what you get, *Amyloid 12*, 88−95.
17. Klein, W. L., Stine, W. B., Jr., and Teplow, D. B. (2004) Small assemblies of unmodified amyloid β-protein are the proximate neurotoxin in Alzheimer's disease, *Neurobiol. Aging 25*, 569−580.
18. El-Agnaf, O. M., Nagala, S., Patel, B. P., and Austen, B. M. (2001) Non-fibrillar oligomeric species of the amyloid ABri peptide, implicated in familial British dementia, are more potent at inducing apoptotic cell death than protofibrils or mature fibrils, *J. Mol. Biol. 310*, 157−168.
19. El-Agnaf, O. M., Mahil, D. S., Patel, B. P., and Austen, B. M. (2000) Oligomerization and toxicity of β-amyloid-42 implicated in Alzheimer's disease, *Biochem. Biophys. Res. Commun. 273*, 1003−1007.
20. Tjernberg, L. O., Naslund, J., Lindqvist, F., Iohansson, J., Karlstrom, A. R., Thyberg, J., Terenius, L., and Nordstedt, C. (1996) Arrest of β-amyloid fibril formation by a pentapeptide ligand, *J. Biol. Chem. 271*, 8545−8548.
21. Balbach, J. J., Ishii, Y., Antzutkin, O. N., Leapman, R. D., Rizzo, N. W., Dyda, F., Reed, J., and Tycko, R. (2000) Amyloid fibril formation by Aβ 16−22, a seven-residue fragment of the Alzheimer's β-amyloid peptide, and structural characterization by solid-state NMR, *Biochemistry 39*, 13748−13759.
22. Findeis, M. A., Musso, G. M., Arico-Muendel, C. C., Benjamin, H. W., Hundal, A. M., Lee, J. J., Chin, J., Kelley, M., Wakefield, J., Hayward, N. J., and Molineaux, S. M. (1999) Modified-peptide inhibitors of amyloid-β-peptide polymerization, *Biochemistry 38*, 6791−6800.
23. Soto, C., Sigurdsson, E. M., Morelli, L., Kumar, R. A., Castano, E. M., and Frangione, B. (1998) β-Sheet breaker peptides inhibit fibrillogenesis in a rat brain model of amyloidosis: Implications for Alzheimer's therapy, *Nat. Med. 4*, 822−826.
24. Zhang, G., Leibowitz, M. J., Sinko, P. J., and Stein, S. (2003) Multiple-peptide conjugates for binding β-amyloid plaques of Alzheimer's disease, *Bioconjugate Chem. 14*, 86−92.
25. Gazit, E. (2002) A possible role for π-stacking in the self-assembly of amyloid fibrils, *FASEB J. 16*, 77−83.
26. Aggeli, A., Bell, M., Boden, N., Keen, J. N., Knowles, P. F., McLeish, T. C., Pitkeathly, M., and Radford, S. E. (1997) Responsive gels formed by the spontaneous self-assembly of peptides into polymeric β-sheet tapes, *Nature 386*, 259−262.
27. Claessens, C. G., and Stoddart, J. F. (1997) Aromatic interactions in self-assembly, *J. Phys. Org. Chem. 10*, 254−272.
28. Burley, S. K., and Petsko, G. A. (1985) Aromatic−aromatic interaction: A mechanism of protein structure stabilization, *Science 229*, 23−28.
29. Hunter, C. A., Lawson, K. R., Perkins, J., and Urch, C. J. (2001) Aromatic interactions, *J. Chem. Soc., Perkin Trans. 2*, 651−669.
30. Tenidis, K., Waldner, M., Bernhagen, J., Fischle, W., Bergmann, M., Weber, M., Merkle, M. L., Voelter, W., Brunner, H., and Kapurniotu, A. (2000) Identification of a penta- and hexapeptide of islet amyloid polypeptide (IAPP) with amyloidogenic and cytotoxic properties, *J. Mol. Biol. 295*, 1055−1071.
31. Azriel, R., and Gazit, E. (2001) Analysis of the minimal amyloid-forming fragment of the islet amyloid polypeptide. An experimental support for the key role of the phenylalanine residue in amyloid formation, *J. Biol. Chem. 276*, 34156−34161.
32. Reches, M., Porat, Y., and Gazit, E. (2002) Amyloid fibril formation by pentapeptide and tetrapeptide fragments of human calcitonin, *J. Biol. Chem. 277*, 35475−35480.
33. Jones, S., Manning, J., Kad, N. M., and Radford, S. E. (2003) Amyloid-forming peptides from 2-microglobulin: Insights into the mechanism of fibril formation *in vitro*, *J. Mol. Biol. 325*, 249−257.
34. Mazor, Y., Gilead, S., Benhar, I., and Gazit, E. (2002) Identification and Characterization of a Novel Molecular-Recognition and Self-Assembly Domain in the Islet Amyloid Polypeptide, *J. Mol. Biol. 322*, 1013−1024.
35. Reches, M., and Gazit, E. (2004) Amyloidogenic Hexapeptide Fragment of Medin: Implications for the Stacking Model of Fibrillization, *Amyloid 11*, 81−89.
36. Naito, A., Kamihira, M., Inoue, R., and Saito, H. (2004) Structural diversity of amyloid fibril formed in human calcitonin as revealed by site-directed ^{13}C solid-state NMR spectroscopy, *Magn. Reson. Chem. 42*, 247−257.
37. Makin, O. S., Atkins, E., Sikorski, P., Johansson, J., and Serpell, L. C. (2005) Molecular basis for amyloid fibril formation and stability, *Proc. Natl. Acad. Sci. U.S.A. 102*, 315−320.
38. Tartaglia, G. G., Cavalli, A., Pellarin, R., and Caflisch, A. (2004) The role of aromaticity, exposed surface, and dipole moment in determining protein aggregation rates, *Protein Sci. 13*, 1939−1941.
39. Zanuy, D., and Nussinov, R. (2003) The sequence dependence of fiber organization. A comparative molecular dynamics study of the islet amyloid polypeptide segments 22−27 and 22−29, *J. Mol. Biol. 329*, 565−584.
40. Zanuy, D., Porat, Y., Gazit, E., and Nussinov, R. (2004) Peptide sequence and amyloid formation: Molecular simulations and experimental study of a human islet amyloid polypeptide fragment and its analogues, *Structure 12*, 439−455.
41. Colombo, G., Daidone, I., Gazit, E., Amadei, A., and Di Nola, A. (2005) Molecular dynamics simulation of the aggregation of the core-recognition motif of the islet amyloid polypeptide in explicit water, *Proteins 59*, 519−527.
42. Haspel, N., Zanuy, D., Ma, B., Wolfson, H., and Nussinov, R. (2005) A comparative study of amyloid fibril formation by residues 15−19 of the human calcitonin hormone: A single β-sheet model with a small hydrophobic core, *J. Mol. Biol. 345*, 1213−1227.
43. Wu, C., Lei, H., and Duan, Y. (2005) The role of Phe in the formation of well-ordered oligomers of amyloidogenic hexapeptide (NFGAIL) observed in molecular dynamics simulations with explicit solvent, *Biophys. J. 88*, 2897−2906.
44. Pawar, A. P., DuBay, K. F., Zurdo, J., Chiti, F., Vendruscolo, M., and Dobson, C. M. (2005) Prediction of "aggregation-prone" and "aggregation susceptible" regions in proteins associated with neurodegenerative diseases, *J. Mol. Biol. 350*, 379−392.
45. Porat, Y., Stepensky, A., Ding, F. X., Naider, F., and Gazit, E. (2003) Completely different amyloidogenic potential of nearly identical peptide fragments, *Biopolymers 69*, 161−164.
46. Porat, Y., Mazor, Y., Efrat, S., and Gazit, E. (2004) Inhibition of islet amyloid polypeptide fibril formation: A potential role for heteroaromatic interactions, *Biochemistry 43*, 14454−14462.
47. Chyan, Y. J., Poeggeler, B., Omar, R. A., Chain, D. G., Frangione, B., Ghiso, J., and Pappolla, M. A. (1999) Potent neuroprotective

properties against the Alzheimer β-amyloid by an endogenous melatonin-related indole structure, indole-3-propionic acid, *J. Biol. Chem. 274*, 21937−21942.
48. Bendheim, P. E., Poeggeler, B., Neria, E., Ziv, V., Pappolla, M. A., and Chain, D. G. (2002) Development of indole-3-propionic acid (OXIGON) for Alzheimer's disease, *J. Mol. Neurosci. 19*, 213−217.
49. Hansen, M. B., Nielsen, S. E., and Berg, K. (1989) Re-examination and further development of a precise and rapid dye method for measuring cell growth/cell kill, *J. Immunol. Methods 119*, 203−210.
50. Jarrett, J. T., Berger, E. P., and Lansbury, P. T., Jr. (1993) The carboxy terminus of the β amyloid protein is critical for the seeding of amyloid formation: Implications for the pathogenesis of Alzheimer's disease, *Biochemistry 32*, 4693−4697.
51. Nanda, V., and Brand, L. (2000) Aromatic interactions in homeodomains contribute to the low quantum yield of a conserved, buried tryptophan, *Proteins 40*, 112−125.
52. Burley, S. K., and Petsko, G. A. (1985) Aromatic−aromatic interaction: A mechanism of protein structure stabilization, *Science 229*, 23−28.
53. Qin, X. R., Abe, H., and Nakanishi, H. (2002) NMR and CD studies on the interaction of Alzheimer β-amyloid peptide (12−28) with β-cyclodextrin, *Biochem. Biophys. Res. Commun. 297*, 1011−1015.
54. Walsh, D. M., Klyubin, I., Fadeeva, J. V., Cullen, W. K., Anwyl, R., Wolfe, M. S., Rowan, M. J., and Selkoe, D. J. (2002) Naturally secreted oligomers of amyloid β protein potently inhibit hippocampal long-term potentiation *in vivo*, *Nature 416*, 535−539.
55. Klein, W. L., Krafft, G. A., and Finch, C. E. (2001) Targeting small Aβ oligomers: The solution to an Alzheimer's disease conundrum? *Trends Neurosci. 24*, 219−224.
56. Cohen, F. E., and Kelly, J. W. (2003) Therapeutic approaches to protein-misfolding diseases, *Nature 426*, 905−909.
57. Gazit, E. (2004) The role of prefibrillar assemblies in the pathogenesis of amyloid diseases, *Drugs Future 29*, 613−619.
58. Jarrett, J. T., and Lansbury, P. T., Jr. (1993) Seeding one-dimensional crystallization of amyloid: A pathogenic mechanism in Alzheimer's disease and scrapie? *Cell 73*, 1055−1058.
59. Naiki, H., Gejyo, F., and Nakakuki, K. (1997) Concentration-dependent inhibitory effects of apolipoprotein E on Alzheimer's β-amyloid fibril formation *in vitro*, *Biochemistry 36*, 6243−6250.
60. De Felice, F. G., Vieira, M. N., Saraiva, L. M., Figueroa-Villar, J. D., Garcia-Abre, J., Liu, R., Chang, L., Klein, W. L., and Ferreira, S. T. (2004) Targeting the neurotoxic species in Alzheimer's disease: Inhibitors of Aβ oligomerization, *FASEB J. 18*, 1366−1372.
61. Ono, K., Yoshiike, Y., Takashima, A., Hasegawa, K., Naiki, H., and Yamada, M. (2003) Potent anti-amyloidogenic and fibril-destabilizing effects of polyphenols in vitro: Implications for the prevention and therapeutics of Alzheimer's disease, *J. Neurochem. 87*, 172−181.
62. Kocisko, D. A., Baron, G. S., Rubenstein, R., Chen, J., Kuizon, S., and Caughey, B. (2003) New inhibitors of scrapie-associated prion protein formation in a library of 2000 drugs and natural products, *J. Virol. 77*, 10288−10294.

BI051525C